Title: Modulation of muscle cell *Insr* and insulin receptor signaling by hyperinsulinemia *in vitro* and *in vivo*

Authors: Haoning Howard Cen, José Diego Botezelli, Su Wang, James D. Johnson*
Affiliation: Department of Cellular and Physiological Sciences, Life Science Institute, University of British Columbia, Vancouver, BC. Canada.
***Address correspondence to:** James D. Johnson, Ph.D., Professor. Diabetes Research Group, Dept. of Cellular and Physiological Sciences & Dept. of Surgery, University of British Columbia, 5358 Life Sciences Building, 2350 Health Sciences Mall, Vancouver, BC, Canada, V6T 1Z3
E-mail: James.D.Johnson@ubc.ca; Fax: (604) 822-2316; Twitter: @JimJohnsonSci
Running title: Hyperinsulinemia-induced insulin resistance
Keywords: insulin, insulin receptor, insulin resistance, skeletal muscle, FOXO

Abstract

Hyperinsulinemia is often viewed as a compensatory mechanism for insulin resistance, but studies have shown that high levels of insulin may also contribute to insulin resistance. The precise mechanisms by which hyperinsulinemia contributes to insulin resistance remain poorly defined. To understand the direct effects of prolonged exposure to excess insulin in muscle cells, we incubated differentiated C2C12 mouse myotubes with elevated insulin for 16 hours, followed by a 6-hour period of serum starvation, before examining key insulin signaling nodes. Using our model, we found that prolonged high insulin treatment significantly increased the phosphorylation of insulin receptor (INSR) and AKT, but not ERK. After serum starvation, acute AKT and ERK signaling stimulated by 0.2 - 20 nM insulin were attenuated. INSR protein levels were significantly downregulated by hyperinsulinemia in an insulin-dose-dependent manner, which resulted in the comparative reduction of acute insulin signaling. Surface INSR was also reduced proportionally to total INSR levels. Mechanistically, we found that both isoforms of *Insr* mRNA were reduced by hyperinsulinemia and implicated the transcription factor FOXO1. Interestingly, 6h serum starvation reversed the effects of high insulin on basal phosphorylation of INSR, AKT and FOXO1, and *Insr* transcription. Finally, we validated our results *in vivo* by determining that INSR levels in mouse skeletal muscle were negatively correlated with circulating insulin. Together, our findings shed light on the mechanisms underlying hyperinsulinemia-induced insulin resistance in muscle cells, which are likely to be relevant in the pathogenesis of type 2 diabetes.

Introduction

Hyperinsulinemia and insulin resistance are cardinal features of type 2 diabetes (T2D) and highly associated with each other. It is a widely held view that insulin resistance is the primary cause of type 2 diabetes and that hyperinsulinemia is a compensatory response (1,2). However, a growing body of evidence suggests the opposite may be true in many cases (3-5). Hyperinsulinemia can be observed prior to insulin resistance in obesity and T2D (6-8) and hyperinsulinemia is the strongest predictor of T2D in long-term studies (9,10). We recently showed that hyperinsulinemia contributes causally to age-dependent insulin resistance in the absence of hyperglycemia (11). Reducing hyperinsulinemia using partial insulin gene knockout prevents and reverses diet-induced obesity in adult mice (11-13). Rodents (14,15), healthy humans (16,17), and people with type 1 diabetes (18) subjected to prolonged insulin administration also have reduced insulin responsiveness independent of hyperglycemia, strongly suggesting that hyperinsulinemia is a self-perpetuating cause of insulin resistance.

The mechanisms by which hyperinsulinemia contributes to insulin resistance remain poorly understood. The insulin receptor (INSR) is a critical component as the starting point of insulin action. It has been reported that diabetic or obese rodent models with hyperinsulinemia and insulin resistance have reduced insulin binding to the liver (19), fat (20) and pancreatic acinar cells (21). The insulin binding defect may be due to INSR downregulation rather than immediate changes in binding affinity, since chronic (2-16 hours), but not acute, high insulin exposure directly reduced insulin binding and INSR protein levels in adipocytes (22) and lymphocytes (23) *in vitro*. However, the molecular mechanisms of INSR down-regulation and post-receptor insulin resistance remain poorly characterized, especially in muscle cells.

In the present study, we employed a model of *in vitro* insulin resistance using a muscle cell line and confirmed our observations *in vivo* using mice with variable hyperinsulinemia. We found that prolonged hyperinsulinemia induced insulin resistance featuring blunted acute AKT and ERK signaling and transcriptional INSR downregulation via FOXO1 activity. Our data illuminate the mechanism by which hyperinsulinemia contributes to insulin resistance in muscle cells.

Results

Hyperinsulinemia induces insulin resistance in muscle cells in vitro

Circulating insulin in humans oscillates in a range between 0.03 nM and 1.9 nM, and fasting insulin less than 0.17 nM is considered normal (24). To establish a muscle cell model of hyperinsulinemia-induced insulin resistance, we incubated differentiated mouse C2C12 myotubes for 16 hours in a physiologically high insulin dose of 2 nM or superphysiologically high dose of

200 nM (Fig. 1A). Insulin levels at the end of this hyperinsulinemia period were confirmed to be hyperinsulinemic (Fig. 1A'). After 6-hour serum starvation, acute insulin signaling was characterized by measuring the phosphorylation of AKT and ERK proteins, which represent two major insulin signaling nodes (25). Since alterations in the basal state of the insulin signal transduction network have also been reported in hyperinsulinemic humans and animals (26), we also measured the effects of hyperinsulinemia on AKT and ERK phosphorylation before and after serum starvation. These experiments showed that total AKT protein levels were significantly downregulated by prolonged 200 nM, but not 2 nM, insulin treatment, while ERK abundance was not significantly changed (Fig. 1C,D). After prolonged 200 nM insulin and before serum starvation, AKT phosphorylation at threonine (T) 308 and serine (S) 473 was significantly elevated, but ERK phosphorylation was unaffected (Fig. 1E,F). Of note, phosphorylation of ERK1/2 was increased by serum starvation alone, as previously reported in other cell types (Fig. 1F)(27). Acute AKT and ERK signaling in the context of 2 nM acute insulin was significantly reduced by hyperinsulinemia treatment in an insulin dose-dependent manner (Fig. 1E,F). We also characterized the insulin dose- and time-dependent signaling in our *in vitro* hyperinsulinemia model (200 nM insulin). Phosphorylation of AKT and ERK1/2 were significantly reduced under 0.2, 2, or 20 nM insulin stimulations (Fig. 2A,B). Together, these results establish a robust muscle cell insulin resistance model induced by hyperinsulinemia and characterized its effects on basal and acute insulin signaling.

Hyperinsulinemia reduces INSR protein abundance but not its phosphorylation or internalization

To better understand the effects of hyperinsulinemia on the earliest stages of insulin signalling, we examined on INSR abundance, phosphorylation, and internalization. Remarkably, we found the total INSR protein abundance was robustly decreased in both hyperinsulinemia groups in an insulin dose-dependent manner (Fig. 3B). Serum starvation also slightly recovered the INSR downregulation in 200 nM insulin group (Fig. 3B). These results clearly demonstrated that hyperinsulinemia can modulate INSR abundance in this cell system.

We also examined INSR tyrosine 1150/1151 autophosphorylation, which is an early step of insulin signaling that recruits IRS and SHC, leading to PI3K-AKT or RAS-ERK activation (25). Before starvation, both hyperinsulinemia groups had increased INSR phosphorylation, suggesting that there was continuous insulin signaling during the high insulin treatments (Fig. 3C). Serum starvation completely reversed INSR hyperphosphorylation (Fig. 3C). While the phosphorylation of INSR had no significant difference after 10 min acute insulin stimulations (Fig. 3C), the dose- and time-dependent insulin signaling revealed slightly increased phosphorylated-to-total INSR

ratio in the 200 nM insulin-treated group under acute insulin stimulations (Fig. 3D). The increased INSR phosphorylation per receptor was offset by the reduced INSR number, leading to a decreased phospho-INSR-to-tubulin ratio (i.e. the overall INSR phosphorylation events per cell) (Fig. 3D). These data indicate that INSR do not have defects in autophosphorylation upon acute insulin stimulation in our system.

Impaired INSR endocytosis has been implicated in insulin resistance (28,29). Basal surface INSR, as well as dose- and time-dependent INSR internalization were examined in our hyperinsulinemia model using a surface biotinylation assay (Fig. 4A). Serum starvation slightly decreased surface-to-total INSR ratio, while hyperinsulinemia had no significant effects (Fig. 4B). Upon acute insulin stimulation, internalized to total INSR ratio did not have evident differences except for a small increase when stimulated by 2 nM insulin (Fig. 4B). Therefore, hyperinsulinemia-induced insulin resistance may be mediated by a reduction in total INSR that results in a proportional reduction in INSR protein at the cell surface. The fraction of INSR internalized during acute insulin signaling is not drastically affected by hyperinsulinemia. Collectively, our experiments suggest that hyperinsulinemia-induced insulin resistance is mediated in large part by a reduction in total INSR, and not by affecting its activity or internalization.

Hyperinsulinemia decreases Insr mRNA via FOXO1 inhibition

One possible cause of INSR downregulation would be the reduced expression of the *Insr* gene (21). To test this hypothesis, we measured the mRNA of *Insr* isoforms A and B (*Insr-A* and *Insr-B*) by qPCR. In our hands, *Insr-A* is the predominant isoform in C2C12 myotubes (Fig. 5A). Both *Insr-A* and *Insr-B* mRNA were equally downregulated after hyperinsulinemia and partially recovered after serum starvation (Fig. 5A), consistent with the change of INSR protein abundance. Interestingly, insulin-like growth factor 1 receptor (*Igfr1*), which has similar structure and signaling as INSR, was also reduced by hyperinsulinemia at the transcriptional level (Fig. 5B). Alteration in *Insr* alternative splicing has been implicated in hyperinsulinemia (30). In our model, the ratio of *Insr-A* and *Insr-B* mRNA was not affected by hyperinsulinemia or serum starvation (Fig. 5C). Our evidence suggests that hyperinsulinemia and serum starvation regulate INSR protein abundance by regulating *Insr* mRNA levels.

Forkhead box protein O1 (FOXO1) is a known transcriptional regulator of the *Insr* gene and is also a key mediator of insulin signaling (31-33). In *Drosophila* and mouse myoblasts, FOXO1 activity is necessary and sufficient to increase *Insr* transcription under serum fasting and reverse this effect in the presence of insulin (32). Therefore, we sought to determine the activity of FOXO1 in our hyperinsulinemic model. Indeed, high insulin inhibited FOXO1 via increased phosphorylation on T24, which is an AKT-associated event known to exclude this protein from

the nucleus and decrease FOXO transcriptional activity (34), but did not affect total FOXO1 abundance (Fig. 5D). T24 phosphorylation of FOXO1 significantly decreased after starvation (Fig. 5D), consistent with our observed effects on AKT phosphorylation and *Insr* transcription. Together, these data strongly suggest that hyperinsulinemia downregulates *Insr* transcription via FOXO1 phosphorylation.

Circulating insulin negatively correlates with INSR level in vivo

To validate our *in vitro* studies, we examined the relationship between *in vivo* insulin concentration and muscle INSR level in mice. As in our previous studies (12), insulin gene dosage was manipulated ($Ins1^{+/+}$;$Ins2^{-/-}$ and $Ins1^{+/-}$;$Ins2^{-/-}$) to generate variance in circulating insulin. The mice were fed with high fat diet (HFD) known to induced pronounced hyperinsulinemia (12,35) or low fat diet (LFD). These experiments showed that INSR protein abundance negatively correlated with both fasting insulin and fasting glucose in the HFD group (Fig. 5A-B). However, the LFD group only had a negative correlation between INSR level and insulin, with no correlation between INSR and glucose (Fig. 5C-D). These data support the concept that insulin, independent from glucose, can negatively regulate INSR levels in skeletal muscle, consistent with our *in vitro* hyperinsulinemia model and our previous *in vivo* data demonstrating improved insulin sensitivity over time in mice with genetically reduced insulin production (11). These data also suggest an interaction between insulin, glucose and INSR that is dependent on the conditions of the HFD.

Discussion

The goal of this study was to explore the mechanisms of hyperinsulinemia-induced insulin resistance in skeletal muscle cells. We demonstrated that prolonged physiological and superphysiological hyperinsulinemia induced a reduction of AKT and ERK signaling. Remarkably, while serum starvation partially reversed the effects of overnight hyperinsulinemia, much of the impaired acute insulin signaling we observed after 16 hours of hyperinsulinemia was sustained after 6 hours of insulin withdrawal and serum starvation, suggesting that long-term molecular changes underlie these differences. The effects of prolonged hyperinsulinemia were dose-dependent from the physiological to the superphysiological range. We demonstrated that the impaired insulin response in our system can be accounted for by INSR downregulation at the transcription level via FOXO1 phosphorylation. We validated our *in vitro* system *in vivo* in mice with varying degrees of diet-induced hyperinsulinemia.

Our *in vitro* cell culture model provided a robust and controlled system for examining the direct effects of excess insulin, and insulin withdrawal, on multiple components of insulin signaling.

Our results are consistent with other *in vitro* cell culture systems designed to examine the effects of hyperinsulinemia. For example, reduced AKT and ERK signaling and INSR abundance were also reported in hyperinsulinemia-treated β-cells (INS1E cell line and rat islets) and enteroendocrine L cells (36,37). The molecular mechanisms mediating the down-regulation of signaling components are unclear, but we speculate that the proteosome may be involved because IGF1 treatment can cause proteasome-dependent downregulation of AKT protein (41). The mechanisms of sustained alterations in AKT and ERK phosphorylation are also not fully understood. In our experiments, there was suppressed AKT and ERK phosphorylation at all time points, suggesting that the insulin resistance we observed was impaired responsiveness consistent with signaling deficiencies at both the receptor level and in post-receptor components (40). Our observations verified the distinct responses to hyperinsulinemia of the bifurcate insulin signaling pathways. Chronic 200 nM insulin treatment preferentially increased basal AKT phosphorylation, but did not increase the basal ERK phosphorylation, which is a result that has also been reported in neurons (38). Diet and hyperinsulinemia-induced insulin resistance is generally considered to be related specifically to AKT phosphorylation. Interestingly, chemical inhibition of AKT pathway, but not ERK pathway, has been reported to protect insulin resistance both *in vitro* and *in vivo* (38,39). Further work is required to understand the interplay between INSR expression and downstream signaling.

The main finding of our study was that that hyperinsulinemia directly reduced *Insr* mRNA in cultured cells, consistent with reports from other cell culture systems (21,42). In a previous study, we observed a ~20% increase in *Insr* mRNA from skeletal muscle samples of *Ins1*$^{+/-}$;*Ins2*$^{-/-}$ mice compared to *Ins1*$^{+/+}$;*Ins2*$^{-/-}$ mice, as well as a trend of a ~50% increase in *Foxo1* mRNA (12). Our *in vivo* data in mice are also consistent with the limited data from human studies. For example, T2D patients with higher fasting insulin were found to have lower *Insr* mRNA expression in skeletal muscle biopsies (43). While relative hyperglycemia can increase *Insr* expression in lymphocyte and cancer cell lines (44,45), high glucose inhibits β-cell *Insr* expression through autocrine insulin action and INSR-FOXO1 signaling (44,45). Interestingly, glucose can only induce insulin resistance in the presence of insulin in cultured hepatocytes, adipocytes and skeletal muscle (20,46,47). Therefore, reduced *Insr* expression by hyperinsulinemia may be a key, independent factor of INSR downregulation and insulin resistance.

Intermittent fasting, time-restricted feeding, caloric restriction, and/or carbohydrate restriction have been shown to have health benefits in diabetes, including reducing hyperinsulinemia, increasing insulin sensitivity, improving β-cell responsiveness, and lowering the levels of circulating glucose (48-50). Several human trials suggest that fasting regimes can be more effective for reducing insulin and increasing insulin sensitivity than they are for reducing glucose

(51,52). By mimicking the low-insulin state, the serum starvation phase of our studies revealed some possible molecular mechanisms of the beneficial effects of fasting, which includes the restoration of protein phosphorylation in insulin signaling pathways and partial recovery of *Insr* transcription and INSR protein. These data hint that many deleterious effects of hyperinsulinemia are reversible but may require a long enough low-insulin period.

The present study has limitations and unanswered questions. We employed a 16-hour insulin incubation instead of more chronic hyperinsulin treatment. The main reason for this is that insulin promotes the further differentiation of C2C12 myotubes (53), meaning that chronic treatment during differentiation would likely introduce unmanageble variance in the muscle cell model. Another limitation to our study is that it was not comprehensive with regards to key insulin signaling nodes. Indeed, hyperinsulinemia has been shown to downregulate other insulin signaling proteins such as IRS1 and IRS2 (54,55). In future studies, it would be interesting to examine the effect of hyperinsulinemia and fasting on other signaling molecules in our model to further dissect the cause of insulin resistance. Besides FOXO1, other transcription factors such as SP1, HMGA1, C/EBPβ, and NUCKS have been shown to regulate *Insr* expression (56-58). For example, HMGA1 is downregulated in diabetes, which inhibits *Insr* as well as *Foxo1* transcription (57). The roles of these other transcriptional regulators in hyperinsulinemia could be investigated in future studies using our system. INSR degradation and proteolysis are also increased by high insulin in lymphocyte and adipocytes (21,22,59). Although *Insr* mRNA and protein cannot be directly compared, the fold reduction of *Insr* mRNA was smaller than fold reduction of INSR protein in our cell model, suggesting that additional mechanisms may be involved in modulating the protein abundance of INSR. In addition to the downregulation of INSR protein abundance, INSR was proportionally internalized with a subtle increase, yet the role and mechanism of this phenomenon remain unknown. The mechanisms of INSR and insulin signaling down-regulation in hyperinsulinemia-induced insulin resistance will require more detailed future investigations.

Despite its inherent reductionism, our *in vitro* model reemphasized the critical and detrimental role of hyperinsulinemia in the development of insulin resistance and T2D. We demonstrated that *in vitro* hyperinsulinemia and serum fasting had profound effects and interactions in regulating AKT and ERK signaling and protein levels, INSR abundance and localization, and transcriptional activities, which provided valuable insights on the molecular mechanisms of insulin resistance. Future additional characterization of the effect of hyperinsulinemism on INSR trafficking, degradation, and detailed post-receptor alterations will provide more insight in the molecular mechanisms of diabetes progression and further highlights dysregulated basal insulin as a direct cause and hallmark of diabetes.

Experimental Procedures

Cell culture

The C2C12 mouse myoblast (ATCC cell line provided by Dr. Brain Rodrigues, University of British Columbia, Vancouver, Canada) was maintained in Dulbecco's modified Eagle's medium (DMEM, Invitrogen) supplemented with 10% (v/v) fetal bovine serum (FBS, Gibco), and 1% penicillin-streptomycin (100 µg/ml; Gibco). For downstream analysis, 8×10^5 cells/well of cells were seeded in 6-well plates and cultured at 37 °C under 5% CO_2. Confluent (90%) myoblasts were differentiated into myotubes by culturing the cells in differentiation medium (DMEM supplemented with 2% horse serum and 1% penicillin-streptomycin) for 10 days. To induce insulin resistance by hyperinsulinemia *in vitro*, C2C12 myotubes were cultured in differentiation medium containing 2 or 200 nM human insulin (Cat.# I9278, Sigma) for 16 hours prior to reaching day 10 (Fig.1A). Insulin concentrations after the 16 h hyperinsulinemia treatment were measured using human insulin RIA kit (Millipore). For serum starvation, myotubes were maintained in serum-free medium (DMEM supplemented with 1% penicillin-streptomycin) for 6 hours. All experiments were repeated with biological replicates using cells in different passages.

Experimental Animals

Animal protocols were approved by the University of British Columbia Animal Care Committee. *Ins1*$^{+/+}$;*Ins2*$^{-/-}$ and *Ins1*$^{+/-}$;*Ins2*$^{-/-}$ mice were randomly assigned to be fed *ad libitum* either a high fat diet (Research Diets D12492, 20% protein, 60% fat, 20% carbohydrate content, energy density 5.21Kcal/g, Brunswick, NJ, US) or low fat diet (Research Diets D12450B, 20% protein 10% fat, 70% carbohydrate content, energy density 3.82Kcal/g, Brunswick, NJ, US) for 4 weeks starting from 8 weeks old. Blood fasting glucose was measured using OneTouch Ultra2 glucose meters (LifeScan Canada Ltd, BC, Canada), and serum fasting insulin were assessed using mouse insulin ELISA kit (Alpco Diagnostics, Salem, NH, USA), following 4-hour fasting.

RNA isolation and quantitative real-time PCR analysis

Before and after serum starvation, total RNA was isolated from both control and high insulin-treated C2C12 myotubes using the RNEasy mini kit (Qiagen). cDNA was generated by reverse transcription using qScript cDNA synthesis kit (Quanta Biosciences, Gaithersburg, MD, USA). Transcript levels of target genes in the equal amount of total cDNA were quantified with SYBR green chemistry (Quanta Biosciences) on a StepOnePlus Real-time PCR System (Applied Biosystems). All data were normalized to *Hprt* by the $2^{-\Delta Ct}$ method. The following primers are used in qPCR: *Insr-A/B* forward 5'-TCCTGAAGGAGCTGGAGGAGT-3', *Insr-A* reverse 5'-CTTTCGGGATGGCCTGG-3', *Insr-B* reverse 5'-TTCGGGATGGCCTACTGTC-3' (60); *Igf1r*

forward 5'-GGCACAACTACTGCTCCAAAGAC-3' and reverse 5'-CTTTATCACCACCACACACT TCTG-3' (60); *Hprt* forward 5'-TCAGTCAACGGGGGACATAAA-3' and reverse 5'-GGGGCTGTACTGCTTAA CCAG-3' (61).

Western blot analyses

C2C12 myotubes or mice skeletal muscle (gastrocnemius) tissues were sonicated in RIPA buffer (50 mM β-glycerol phosphate, 10 mM HEPES, 1% Triton X-100, 70 mM NaCl, 2 mM EGTA, 1 mM Na_3VO_4, and 1 mM NaF) supplemented with complete mini protease inhibitor cocktail (Roche, Laval, QC), and lysates were resolved by SDS-PAGE. Proteins were then transferred to PVDF membranes (BioRad, CA) and probed with antibodies against p-ERK1/2 (Thr202/Tyr204) (1:1000, Cat. #4370), ERK1/2 (1:1000, Cat. #4695), p-AKT (Ser473) (1:1000, Cat. #9271), p-AKT (Thr308) (1:1000, Cat. #9275), AKT (1:1000, Cat. #9272), INSR-β subunit (1:1000, Cat. #3020S), p-INSRβ (Tyr1150/1151) (1:1000, Cat. #3024), FOXO1 (1:1000, Cat. #2880), p-FOXO1 (Thr24) (1:1000, Cat. #9464), all from Cell Signalling (CST), and β-tubulin (1:2000, Cat. #T0198, Sigma). The signals were detected by secondary HRP-conjugated antibodies (Anti-mouse, Cat. #7076; Anti-rabbit, Cat. #7074; CST) and Pierce ECL Western Blotting Substrate (Thermo Fisher Scientific). Protein band intensities were quantified with Image Studio Lite software (LI-COR).

Surface Protein Biotinylation Assay

Biotinylation of surface proteins was performed as previously described(62) with modifications (Fig. 5A). In brief, cells were incubated with cell-impermeable EZ-Link-NHS-SS-biotin (300 μg/ml in PBS; Pierce) at 37°C for 2 min. Cells were then immediately placed on ice and washed with ice-cold 50 mM Tris-buffered saline (TBS) to remove excess biotin. For isolating surface proteins, cells were washed using ice-cold PBS and lysed in complete RIPA buffer (supplemented with cOmplete mini protease inhibitor cocktail (Roche, Laval, QC) and Na_3VO_4). For detecting internalized proteins, cells were washed with PBS and incubated in serum-free medium supplemented with 0.2, 2 or 20 nM insulin at 37°C to stimulate INSR internalization. After certain time periods, cells were placed on ice, washed with ice-cold PBS, incubated with Glutathione solution (50 mM glutathione, 75 mM NaCl, 1 mM EDTA, 1% BSA, 75 mM NaOH) for 20 min to strip remaining surface biotin, washed with excess PBS, and lysed in complete RIPA buffer. Lysates were quantitated and incubated with NeutrAvidin beads (Pierce) overnight at 4 °C to isolate biotinylated surface or internalized proteins. Biotinylated proteins were eluted from the NeutrAvidin beads by boiling in Blue Loading Buffer (CST) containing 50 mM DTT for 5 min. Surface or internalized INSR in eluent and total INSR in lysates were detected in Western blot analysis.

Statistics

Data were presented as mean ± SEM in addition to the individual data points. All data were analyzed using R Studio 3.4.1. A significance level of adjusted $p < 0.05$ was used throughout. All western blot quantifications (protein band intensity) were analyzed using linear regression modeling (63). Linear mixed effect models (R package – lme4) were fitted using restricted maximum likelihood (63,64). Predictor variables were included as fixed effects and sample IDs were included as random effects. Mixed effect modeling was used to account for repeated sample measurements and missing data (63). Where the random effect was not significant, linear fixed effect modeling was used. Heteroscedasticity and normality of residuals were analyzed used Levene's test and the Shapiro–Wilk test, respectively. Predictor variables, insulin treatment (overnight and acute) and time, were treated as ordinal factors and continuous factor, respectively. The outcome variable, protein band intensity, was treated as a continuous factor and log-transformed when residuals are not homoscedastic and/or normally distributed. Multiple comparison p-values were adjusted using the Tukey method.

Acknowledgments: We acknowledge Dr. Brain Rodrigues for providing the C2C12 cells. We thank our colleagues Xiaoke Hu and Leanne Beet for performing the RIA insulin measurement.

Contributions: HC designed the study, performed all experiments except the high-fat feeding, analyzed data and wrote the manuscript. JDB performed *in vivo* high fat feeding and analyzed the related data. SW performed statistical analysis and edited the manuscript. JDJ designed the study, supervised the research and edited the manuscript. JDJ is the ultimate guarantor of this work.

Funding: This study was funded by a CIHR Operating Grant to JDJ.

Conflict of interest: The authors declare that they have no conflicts of interest with the contents of this article.

References

1. Defronzo RA. Banting Lecture. From the triumvirate to the ominous octet: a new paradigm for the treatment of type 2 diabetes mellitus. *Diabetes*. 2009;58(4):773-795.
2. Prentki M, Nolan CJ. Islet beta cell failure in type 2 diabetes. *J Clin Invest*. 2006;116(7):1802-1812.
3. Corkey BE. Banting lecture 2011: hyperinsulinemia: cause or consequence? *Diabetes*. 2012;61(1):4-13.
4. Shanik MH, Xu Y, Skrha J, Dankner R, Zick Y, Roth J. Insulin resistance and hyperinsulinemia: is hyperinsulinemia the cart or the horse? *Diabetes Care*. 2008;31 Suppl 2:S262-268.
5. Page MM, Johnson JD. Mild Suppression of Hyperinsulinemia to Treat Obesity and Insulin Resistance. *Trends Endocrinol Metab*. 2018;29(6):389-399.
6. Le Stunff C, Bougneres P. Early changes in postprandial insulin secretion, not in insulin sensitivity, characterize juvenile obesity. *Diabetes*. 1994;43(5):696-702.
7. Spadaro L, Alagona C, Palermo F, Piro S, Calanna S, Parrinello G, Purrello F, Rabuazzo AM. Early phase insulin secretion is increased in subjects with normal fasting glucose and metabolic syndrome: a premature feature of beta-cell dysfunction. *Nutr Metab Cardiovasc Dis*. 2011;21(3):206-212.
8. Trico D, Natali A, Arslanian S, Mari A, Ferrannini E. Identification, pathophysiology, and clinical implications of primary insulin hypersecretion in nondiabetic adults and adolescents. *JCI Insight*. 2018;3(24).
9. Dankner R, Chetrit A, Shanik MH, Raz I, Roth J. Basal state hyperinsulinemia in healthy normoglycemic adults heralds dysglycemia after more than two decades of follow up. *Diabetes Metab Res Rev*. 2012;28(7):618-624.
10. Zimmet PZ, Collins VR, Dowse GK, Knight LT. Hyperinsulinaemia in youth is a predictor of type 2 (non-insulin-dependent) diabetes mellitus. *Diabetologia*. 1992;35(6):534-541.
11. Templeman NM, Flibotte S, Chik JHL, Sinha S, Lim GE, Foster LJ, Nislow C, Johnson JD. Reduced Circulating Insulin Enhances Insulin Sensitivity in Old Mice and Extends Lifespan. *Cell Rep*. 2017;20(2):451-463.
12. Mehran AE, Templeman NM, Brigidi GS, Lim GE, Chu KY, Hu X, Botezelli JD, Asadi A, Hoffman BG, Kieffer TJ, Bamji SX, Clee SM, Johnson JD. Hyperinsulinemia drives diet-induced obesity independently of brain insulin production. *Cell Metab*. 2012;16(6):723-737.
13. Page MM, Skovso S, Cen H, Chiu AP, Dionne DA, Hutchinson DF, Lim GE, Szabat M, Flibotte S, Sinha S, Nislow C, Rodrigues B, Johnson JD. Reducing insulin via conditional partial gene ablation in adults reverses diet-induced weight gain. *FASEB J*. 2018;32(3):1196-1206.

14. Hamza SM, Sung MM, Gao F, Soltys CM, Smith NP, MacDonald PE, Light PE, Dyck JR. Chronic insulin infusion induces reversible glucose intolerance in lean rats yet ameliorates glucose intolerance in obese rats. *Biochim Biophys Acta Gen Subj*. 2017;1861(2):313-322.
15. Yang X, Mei S, Gu H, Guo H, Zha L, Cai J, Li X, Liu Z, Cao W. Exposure to excess insulin (glargine) induces type 2 diabetes mellitus in mice fed on a chow diet. *J Endocrinol*. 2014;221(3):469-480.
16. Marangou AG, Weber KM, Boston RC, Aitken PM, Heggie JC, Kirsner RL, Best JD, Alford FP. Metabolic consequences of prolonged hyperinsulinemia in humans. Evidence for induction of insulin insensitivity. *Diabetes*. 1986;35(12):1383-1389.
17. Del Prato S, Leonetti F, Simonson DC, Sheehan P, Matsuda M, DeFronzo RA. Effect of sustained physiologic hyperinsulinaemia and hyperglycaemia on insulin secretion and insulin sensitivity in man. *Diabetologia*. 1994;37(10):1025-1035.
18. Gregory JM, Smith TJ, Slaughter JC, Mason HR, Hughey CC, Smith MS, Kandasamy B, Greeley SAW, Philipson LH, Naylor RN, Letourneau LR, Abumrad NN, Cherrington AD, Moore DJ. Iatrogenic Hyperinsulinemia, Not Hyperglycemia, Drives Insulin Resistance in Type 1 Diabetes as Revealed by Comparison to GCK-MODY (MODY2). *Diabetes*. 2019.
19. Soll AH, Kahn CR, Neville DM. Insulin binding to liver plasm membranes in the obese hyperglycemic (ob/ob) mouse. Demonstration of a decreased number of functionally normal receptors. *J Biol Chem*. 1975;250(12):4702-4707.
20. Garvey WT, Olefsky JM, Marshall S. Insulin receptor down-regulation is linked to an insulin-induced postreceptor defect in the glucose transport system in rat adipocytes. *J Clin Invest*. 1985;76(1):22-30.
21. Okabayashi Y, Maddux BA, McDonald AR, Logsdon CD, Williams JA, Goldfine ID. Mechanisms of insulin-induced insulin-receptor downregulation. Decrease of receptor biosynthesis and mRNA levels. *Diabetes*. 1989;38(2):182-187.
22. Ronnett GV, Knutson VP, Lane MD. Insulin-induced down-regulation of insulin receptors in 3T3-L1 adipocytes. Altered rate of receptor inactivation. *J Biol Chem*. 1982;257(8):4285-4291.
23. Gavin JR, Roth J, Neville DM, de Meyts P, Buell DN. Insulin-dependent regulation of insulin receptor concentrations: a direct demonstration in cell culture. *Proc Natl Acad Sci U S A*. 1974;71(1):84-88.
24. Melmed S, Polonsky KS, Larsen PR, Kronenberg HM. Williams Textbook of Endocrinology. 13th ed: Elsevier Saunders.
25. Boucher J, Kleinridders A, Kahn CR. Insulin receptor signaling in normal and insulin-resistant states. *Cold Spring Harb Perspect Biol*. 2014;6(1).

26. Fröjdö S, Vidal H, Pirola L. Alterations of insulin signaling in type 2 diabetes: a review of the current evidence from humans. *Biochim Biophys Acta*. 2009;1792(2):83-92.
27. Morikawa Y, Ueyama E, Senba E. Fasting-induced activation of mitogen-activated protein kinases (ERK/p38) in the mouse hypothalamus. *J Neuroendocrinol*. 2004;16(2):105-112.
28. Jochen AL, Berhanu P, Olefsky JM. Insulin Internalization and Degradation in Adipocytes from Normal and Type-Ii Diabetic Subjects. *J Clin Endocr Metab*. 1986;62(2):268-274.
29. Trischitta V, Gullo D, Squatrito S, Pezzino V, Goldfine ID, Vigneri R. Insulin Internalization into Monocytes Is Decreased in Patients with Type-Ii Diabetes-Mellitus. *J Clin Endocr Metab*. 1986;62(3):522-528.
30. Sbraccia P, D'Adamo M, Leonetti F, Caiola S, Iozzo P, Giaccari A, Buongiorno A, Tamburrano G. Chronic primary hyperinsulinaemia is associated with altered insulin receptor mRNA splicing in muscle of patients with insulinoma. *Diabetologia*. 1996;39(2):220-225.
31. Orengo DJ, Aguadé M, Juan E. Characterization of dFOXO binding sites upstream of the Insulin Receptor P2 promoter across the Drosophila phylogeny. *Plos One*. 2017;12(12):e0188357.
32. Puig O, Tjian R. Transcriptional feedback control of insulin receptor by dFOXO/FOXO1. *Genes Dev*. 2005;19(20):2435-2446.
33. Ni YG, Wang N, Cao DJ, Sachan N, Morris DJ, Gerard RD, Kuro-O M, Rothermel BA, Hill JA. FoxO transcription factors activate Akt and attenuate insulin signaling in heart by inhibiting protein phosphatases. *Proc Natl Acad Sci U S A*. 2007;104(51):20517-20522.
34. Nakae J, Kitamura T, Ogawa W, Kasuga M, Accili D. Insulin regulation of gene expression through the forkhead transcription factor Foxo1 (Fkhr) requires kinases distinct from Akt. *Biochemistry*. 2001;40(39):11768-11776.
35. El Akoum S, Lamontagne V, Cloutier I, Tanguay JF. Nature of fatty acids in high fat diets differentially delineates obesity-linked metabolic syndrome components in male and female C57BL/6J mice. *Diabetol Metab Syndr*. 2011;3.
36. Rachdaoui N, Polo-Parada L, Ismail-Beigi F. Prolonged Exposure to Insulin Inactivates Akt and Erk1/2 and Increases Pancreatic Islet and INS1E beta-Cell Apoptosis. *J Endocr Soc*. 2019;3(1):69-90.
37. Lim GE, Huang GJ, Flora N, LeRoith D, Rhodes CJ, Brubaker PL. Insulin regulates glucagon-like peptide-1 secretion from the enteroendocrine L cell. *Endocrinology*. 2009;150(2):580-591.
38. Kim B, McLean LL, Philip SS, Feldman EL. Hyperinsulinemia induces insulin resistance in dorsal root ganglion neurons. *Endocrinology*. 2011;152(10):3638-3647.

39. Liu HY, Hong T, Wen GB, Han J, Zuo D, Liu Z, Cao W. Increased basal level of Akt-dependent insulin signaling may be responsible for the development of insulin resistance. *Am J Physiol Endocrinol Metab*. 2009;297(4):E898-906.
40. Kahn CR. Insulin resistance, insulin insensitivity, and insulin unresponsiveness: a necessary distinction. *Metabolism*. 1978;27(12 Suppl 2):1893-1902.
41. Adachi M, Katsumura KR, Fujii K, Kobayashi S, Aoki H, Matsuzaki M. Proteasome-dependent decrease in Akt by growth factors in vascular smooth muscle cells. *FEBS Lett*. 2003;554(1-2):77-80.
42. Zhang Z, Li X, Liu G, Gao L, Guo C, Kong T, Wang H, Gao R, Wang Z, Zhu X. High insulin concentrations repress insulin receptor gene expression in calf hepatocytes cultured in vitro. *Cell Physiol Biochem*. 2011;27(6):637-640.
43. Palsgaard J, Brøns C, Friedrichsen M, Dominguez H, Jensen M, Storgaard H, Spohr C, Torp-Pedersen C, Borup R, De Meyts P, Vaag A. Gene expression in skeletal muscle biopsies from people with type 2 diabetes and relatives: differential regulation of insulin signaling pathways. *Plos One*. 2009;4(8):e6575.
44. Martinez SC, Cras-Méneur C, Bernal-Mizrachi E, Permutt MA. Glucose regulates Foxo1 through insulin receptor signaling in the pancreatic islet beta-cell. *Diabetes*. 2006;55(6):1581-1591.
45. Briata P, Briata L, Gherzi R. Glucose starvation and glycosylation inhibitors reduce insulin receptor gene expression: characterization and potential mechanism in human cells. *Biochem Biophys Res Commun*. 1990;169(2):397-405.
46. Liu HY, Cao SY, Hong T, Han J, Liu Z, Cao W. Insulin is a stronger inducer of insulin resistance than hyperglycemia in mice with type 1 diabetes mellitus (T1DM). *J Biol Chem*. 2009;284(40):27090-27100.
47. Ciaraldi TP, Abrams L, Nikoulina S, Mudaliar S, Henry RR. Glucose transport in cultured human skeletal muscle cells. Regulation by insulin and glucose in nondiabetic and non-insulin-dependent diabetes mellitus subjects. *J Clin Invest*. 1995;96(6):2820-2827.
48. Mattson MP, Longo VD, Harvie M. Impact of intermittent fasting on health and disease processes. *Ageing Res Rev*. 2017;39:46-58.
49. Patterson RE, Sears DD. Metabolic Effects of Intermittent Fasting. *Annu Rev Nutr*. 2017;37:371-393.
50. Nuttall FQ, Almokayyad RM, Gannon MC. Comparison of a carbohydrate-free diet vs. fasting on plasma glucose, insulin and glucagon in type 2 diabetes. *Metabolism*. 2015;64(2):253-262.

51. Sutton EF, Beyl R, Early KS, Cefalu WT, Ravussin E, Peterson CM. Early Time-Restricted Feeding Improves Insulin Sensitivity, Blood Pressure, and Oxidative Stress Even without Weight Loss in Men with Prediabetes. *Cell Metab*. 2018;27(6):1212-1221 e1213.
52. Williams KV, Mullen ML, Kelley DE, Wing RR. The effect of short periods of caloric restriction on weight loss and glycemic control in type 2 diabetes. *Diabetes Care*. 1998;21(1):2-8.
53. Sumitani S, Goya K, Testa JR, Kouhara H, Kasayama S. Akt1 and Akt2 differently regulate muscle creatine kinase and myogenin gene transcription in insulin-induced differentiation of C2C12 myoblasts. *Endocrinology*. 2002;143(3):820-828.
54. Kubota T, Inoue M, Kubota N, Takamoto I, Mineyama T, Iwayama K, Tokuyama K, Moroi M, Ueki K, Yamauchi T, Kadowaki T. Downregulation of macrophage Irs2 by hyperinsulinemia impairs IL-4-indeuced M2a-subtype macrophage activation in obesity. *Nat Commun*. 2018;9(1):4863.
55. Pirola L, Bonnafous S, Johnston AM, Chaussade C, Portis F, Van Obberghen E. Phosphoinositide 3-kinase-mediated reduction of insulin receptor substrate-1/2 protein expression via different mechanisms contributes to the insulin-induced desensitization of its signaling pathways in L6 muscle cells. *J Biol Chem*. 2003;278(18):15641-15651.
56. Foti D, Iuliano R, Chiefari E, Brunetti A. A nucleoprotein complex containing Sp1, C/EBP beta, and HMGI-Y controls human insulin receptor gene transcription. *Mol Cell Biol*. 2003;23(8):2720-2732.
57. Foti D, Chiefari E, Fedele M, Iuliano R, Brunetti L, Paonessa F, Manfioletti G, Barbetti F, Brunetti A, Croce CM, Fusco A. Lack of the architectural factor HMGA1 causes insulin resistance and diabetes in humans and mice. *Nat Med*. 2005;11(7):765-773.
58. Qiu B, Shi X, Wong ET, Lim J, Bezzi M, Low D, Zhou Q, Akıncılar SC, Lakshmanan M, Swa HL, Tham JM, Gunaratne J, Cheng KK, Hong W, Lam KS, Ikawa M, Guccione E, Xu A, Han W, Tergaonkar V. NUCKS is a positive transcriptional regulator of insulin signaling. *Cell Rep*. 2014;7(6):1876-1886.
59. Mayer CM, Belsham DD. Central insulin signaling is attenuated by long-term insulin exposure via insulin receptor substrate-1 serine phosphorylation, proteasomal degradation, and lysosomal insulin receptor degradation. *Endocrinology*. 2010;151(1):75-84.
60. Rowzee AM, Ludwig DL, Wood TL. Insulin-like growth factor type 1 receptor and insulin receptor isoform expression and signaling in mammary epithelial cells. *Endocrinology*. 2009;150(8):3611-3619.

61. Zhang J, Tang H, Zhang Y, Deng R, Shao L, Liu Y, Li F, Wang X, Zhou L. Identification of suitable reference genes for quantitative RT-PCR during 3T3-L1 adipocyte differentiation. *Int J Mol Med*. 2014;33(5):1209-1218.
62. Tseng LT, Lin CL, Tzen KY, Chang SC, Chang MF. LMBD1 protein serves as a specific adaptor for insulin receptor internalization. *J Biol Chem*. 2013;288(45):32424-32432.
63. Harrison XA, Donaldson L, Correa-Cano ME, Evans J, Fisher DN, Goodwin CED, Robinson BS, Hodgson DJ, Inger R. A brief introduction to mixed effects modelling and multi-model inference in ecology. *PeerJ*. 2018;6:e4794.
64. Bates D, Machler M, Bolker BM, Walker SC. Fitting Linear Mixed-Effects Models Using lme4. *J Stat Softw*. 2015;67(1):1-48.

Figure Legends

Figure 1. Basal and acute insulin signaling in an *in vitro* hyperinsulinemia-induced insulin resistance model. (A) The workflow of C2C12 myotube differentiation, high insulin treatment and serum starvation. Differentiated myotubes were cultured in control (0 nM insulin) or hyperinsulinemic (2 or 200 nM insulin) medium for 16 hours and were analyzed before and after serum starvation. **(A')** The insulin concentration in the medium at the end of 16-hour high insulin treatment (n=3). **(B)** Representative western blot images of phospho-AKT (T308, S473), total AKT, phospho-ERK1/2, and total ERK1/2. **(C)** Total AKT and **(D)** total ERK abundance under high insulin treatments before starvation (BS) and after starvation (AS). **(E)** phospho-AKT (T308, S473) and **(F)** phospho-ERK1/2 measurements before starvation (BS), after starvation (AS), and stimulated by 0.2 or 2 nM insulin for 10 min after serum starvation. (n=6-9; $^{\#}$ effect of hyperinsulinemia, $^{\$}$ effect of starvation, $^{\&}$ effect of acute insulin, × interaction between two factors, mixed effect model).

Figure 2. Insulin dose- and time-depend acute insulin signaling in the hyperinsulinemia-induced insulin resistance model. Myotubes cultured in control (0 nM insulin) or hyperinsulinemic (200 nM insulin) medium were stimulated with acute 0.2, 2 or 20 nM insulin for 1, 5, 10, 15 or 30 min after serum starvation. **(A)** phospho-AKT (T308, S473) and **(B)** phospho-ERK1/2 was measured. (n=4; $^{\#}$ effect of hyperinsulinemia, $^{\&}$ effect of acute insulin, × interaction between two factors, mixed effect model).

Figure 3. Effects of hyperinsulinemia and serum starvation on INSR abundance and phosphorylation. (A) Representative western blot images of phospho-INSR (Y1150/1151) and total INSR. **(B)** The level of total INSR protein before or after serum starvation (n=4-6). **(C)** phospho-INSR (T308, S473) measurements before starvation (BS), after starvation (AS), and stimulated by 0.2 or 2 nM insulin for 10 min after serum starvation (n=4-6). **(D)** Insulin dose- and time-dependent INSR phosphorylation after serum starvation (n=4). ($^{\#}$ effect of hyperinsulinemia, $^{\$}$ effect of starvation, $^{\&}$ effect of acute insulin, × interaction between two factors, mixed effect model).

Figure 4. Effects of *in vitro* hyperinsulinemia on INSR internalization. (A) Scheme of surface biotinylation assay to measure surface or internalized INSR. Internalized INSR in isolated proteins is detected by western blots. **(B)** The ratio of surface to total INSR ((n = 3 in BS group, n = 10 in AS group). **(C)** The ratio of internalized to total INSR (n = 4). ($^{\#}$ effect of hyperinsulinemia, $^{\$}$ effect of starvation, × interaction between two factors, mixed effect model).

Figure 5. Effects of prolonged hyperinsulinemia and starvation on *Insr* transcription and FOXO1 phosphorylation *in vitro*. (A) The mRNA levels of *Insr* isoform A or B *(Insr-A or B)* before and after starvation (BS and AS) assessed by qPCR. **(B)** *Igf1r* mRNA level. **(C)** The ratio of *Insr-A* to *Insr-B* mRNA. (n=5) **(D)** Total and T24 phosphorylation of FOXO1 (n = 3 in BS group, n = 10 in AS group) ($^{\#}$ effect of hyperinsulinemia, $^{\$}$ effect of starvation, × interaction between two factors, mixed effect model).

Figure 6. *In vivo* correlation between INSR abundance and fasting insulin or glucose in mouse skeletal muscle. (A) INSR and fasting insulin in LFD-fed mice. **(B)** INSR and glucose in LFD-fed mice. **(C)** INSR and fasting insulin in HFD-fed mice. **(D)** INSR and glucose in HFD-fed mice. (n = 7-11)

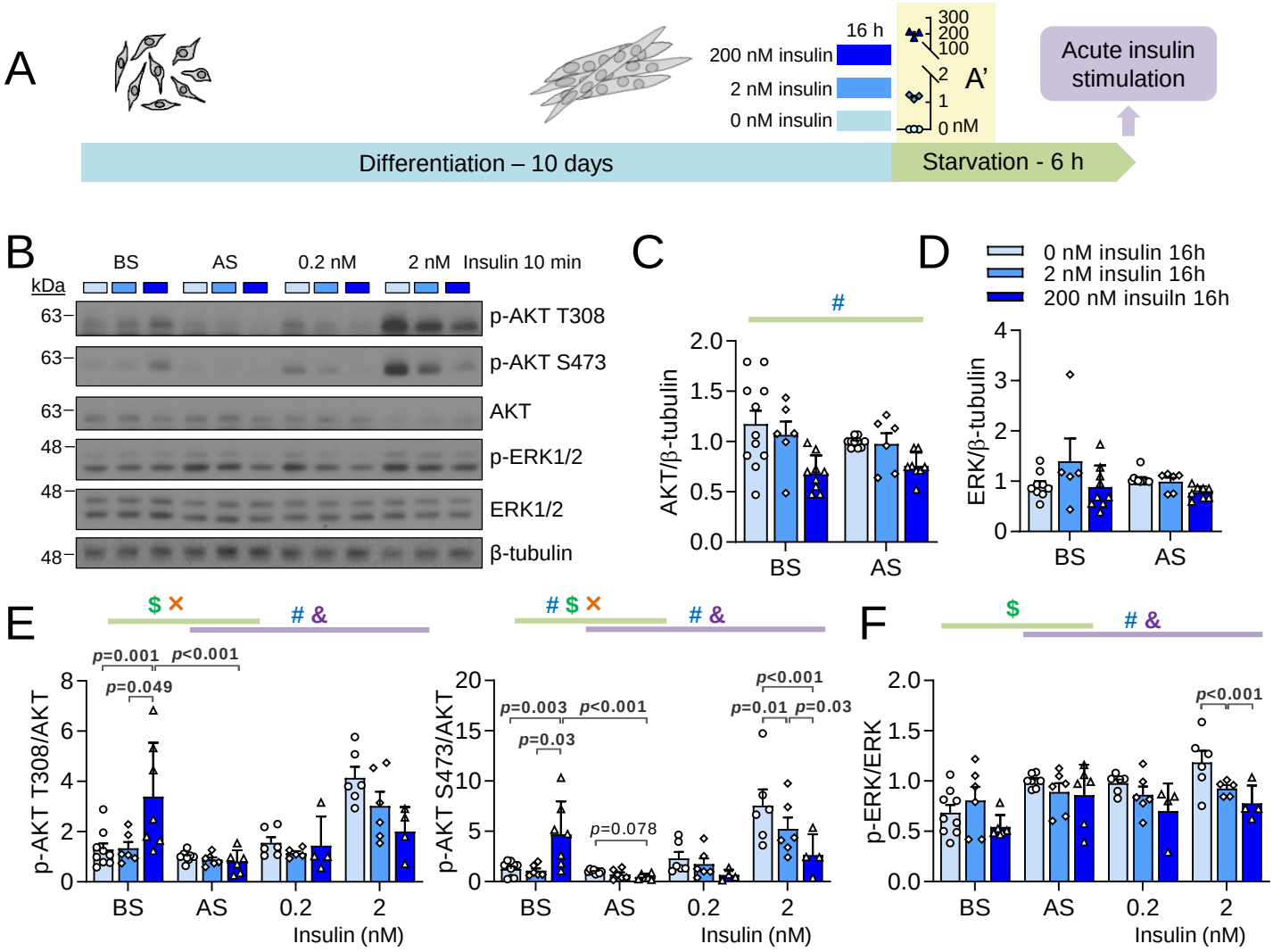

Figure 1. Basal and acute insulin signaling in an *in vitro* hyperinsulinemia-induced insulin resistance model.

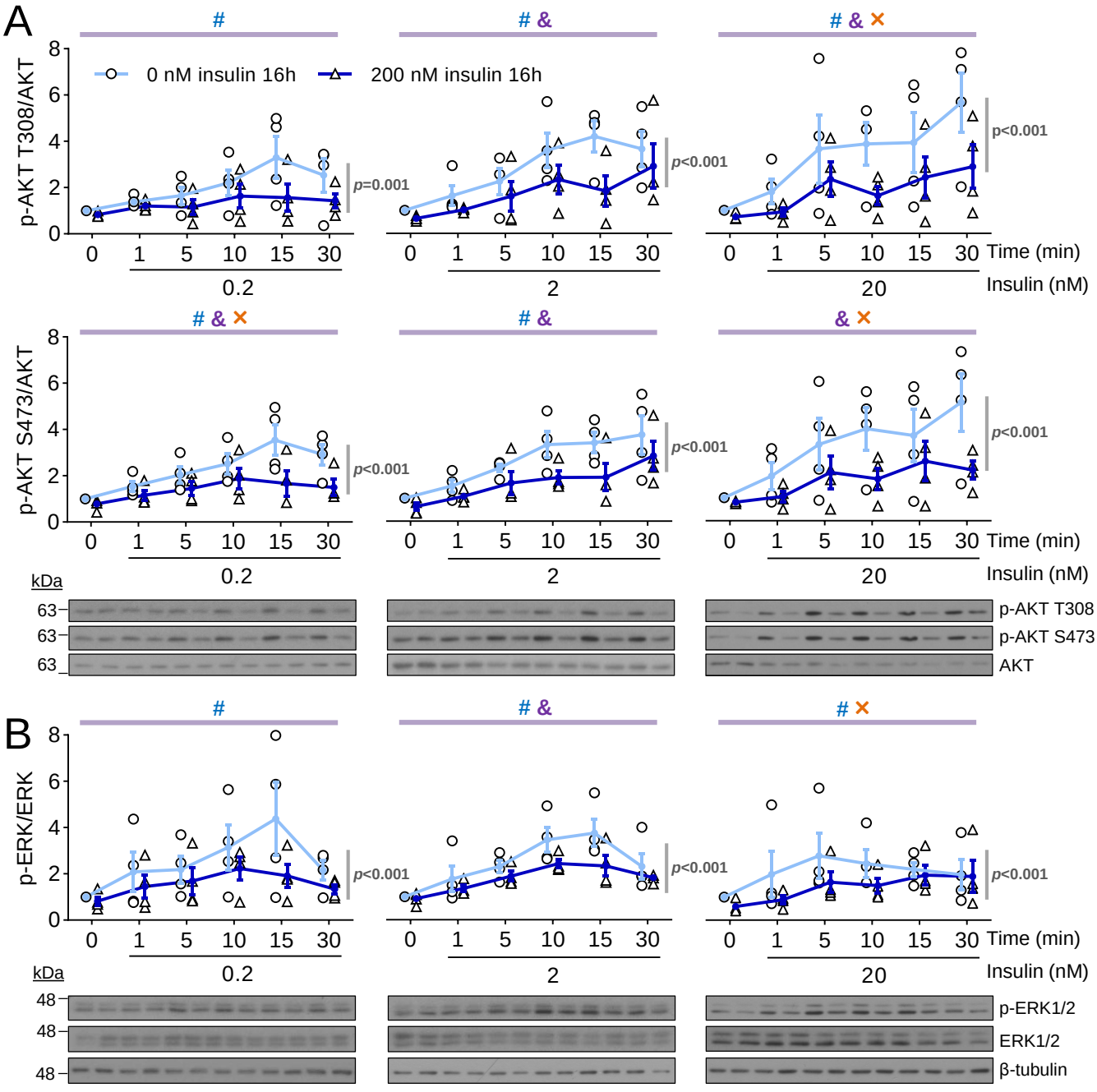

Figure 2. Insulin dose- and time-depend acute insulin signaling in the hyperinsulinemia-induced insulin resistance model.

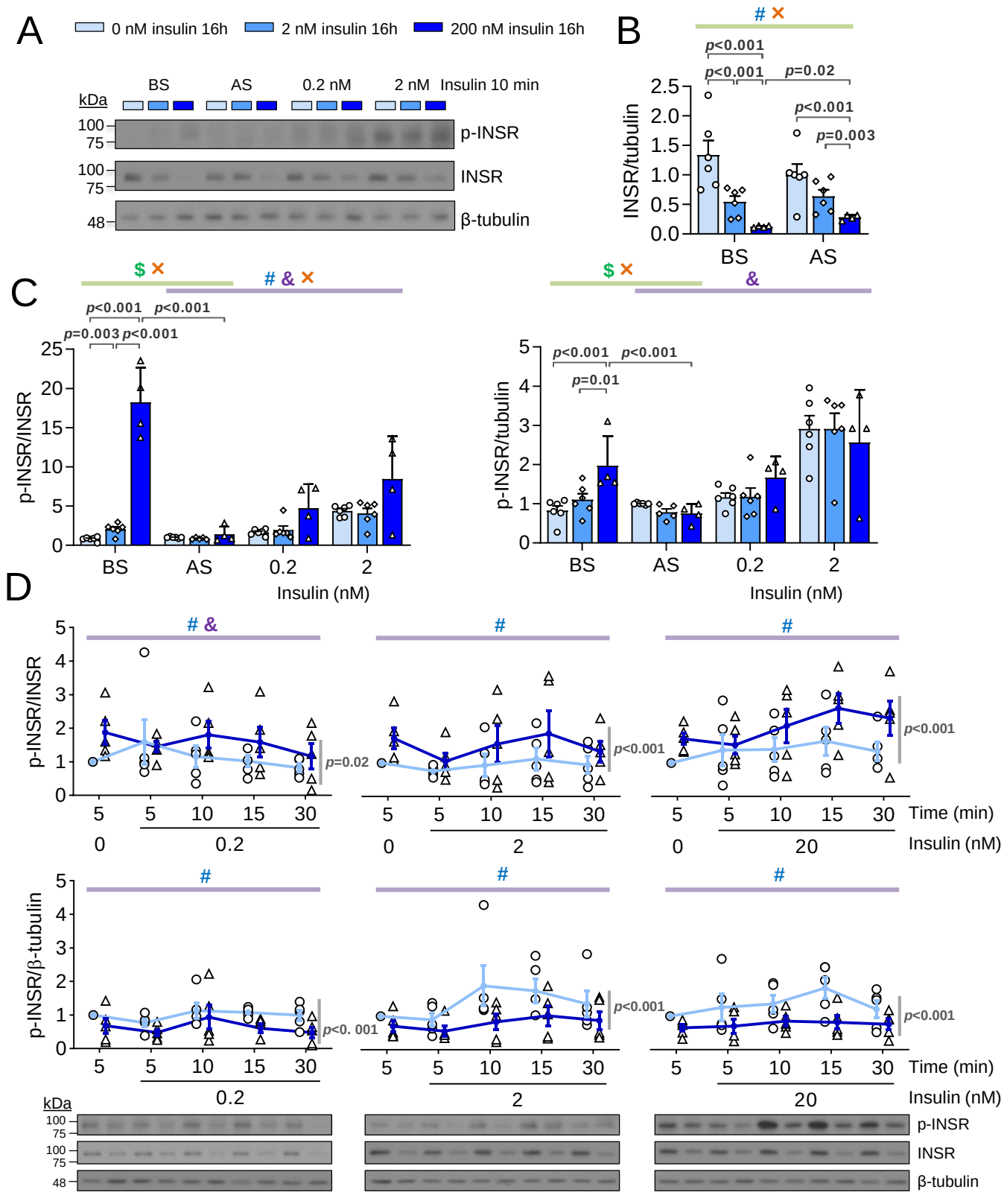

Figure 3. Effects of hyperinsulinemia and serum starvation on INSR abundance and phosphorylation .

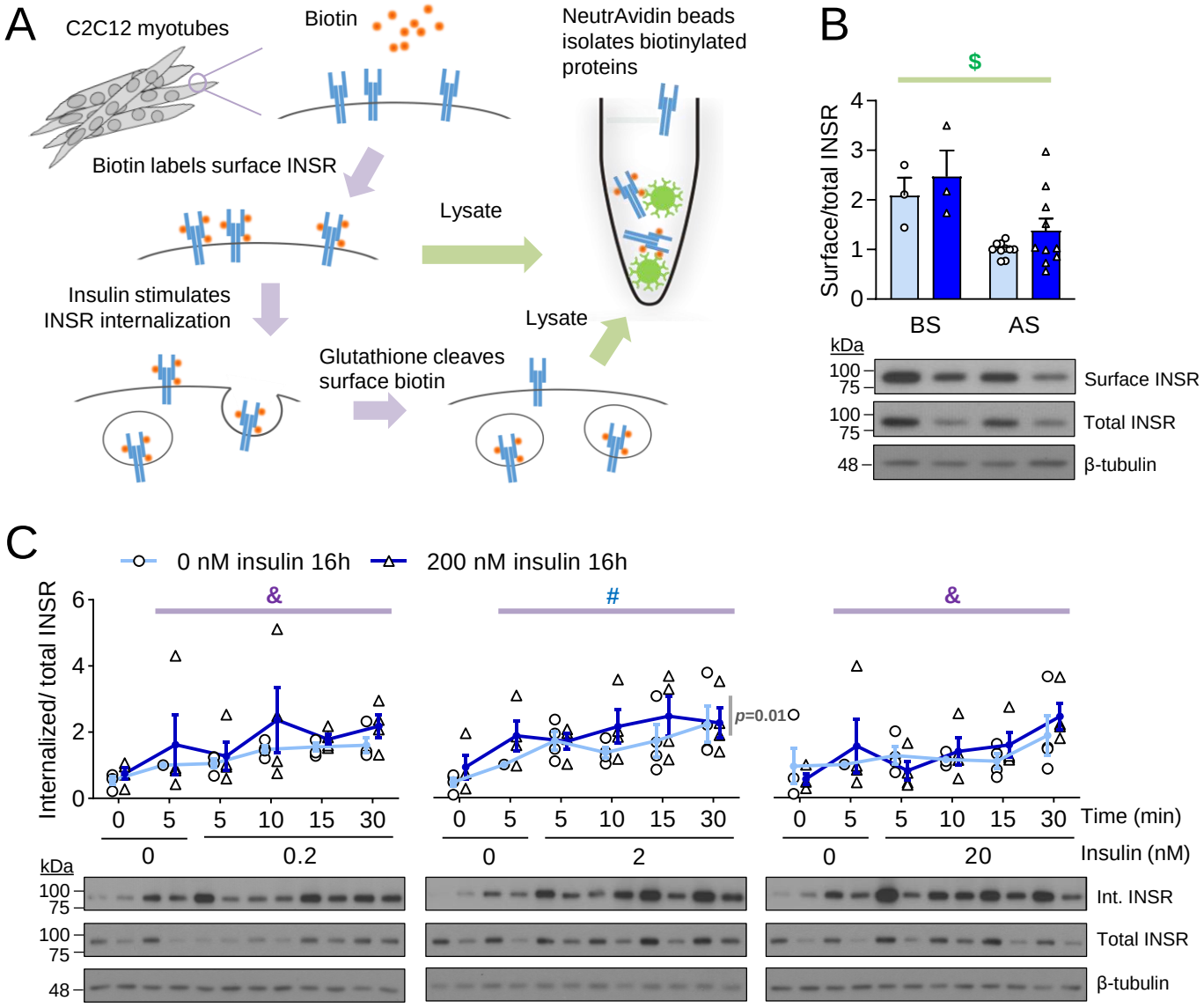

Figure 4. Effects of *in vitro* hyperinsulinemia on INSR internalization.

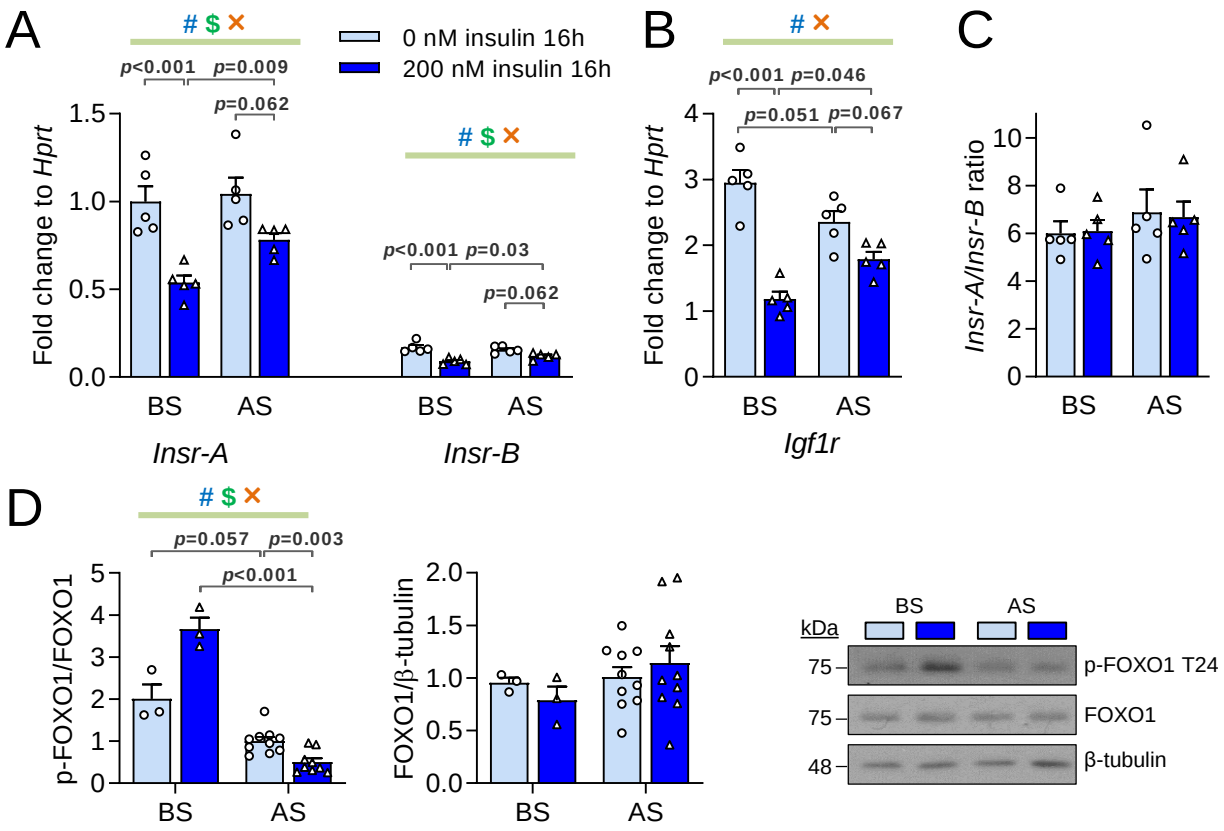

Figure 5. Effects of prolonged hyperinsulinemia and starvation on *Insr* transcription and FOXO1 phosphorylation *in vitro*.

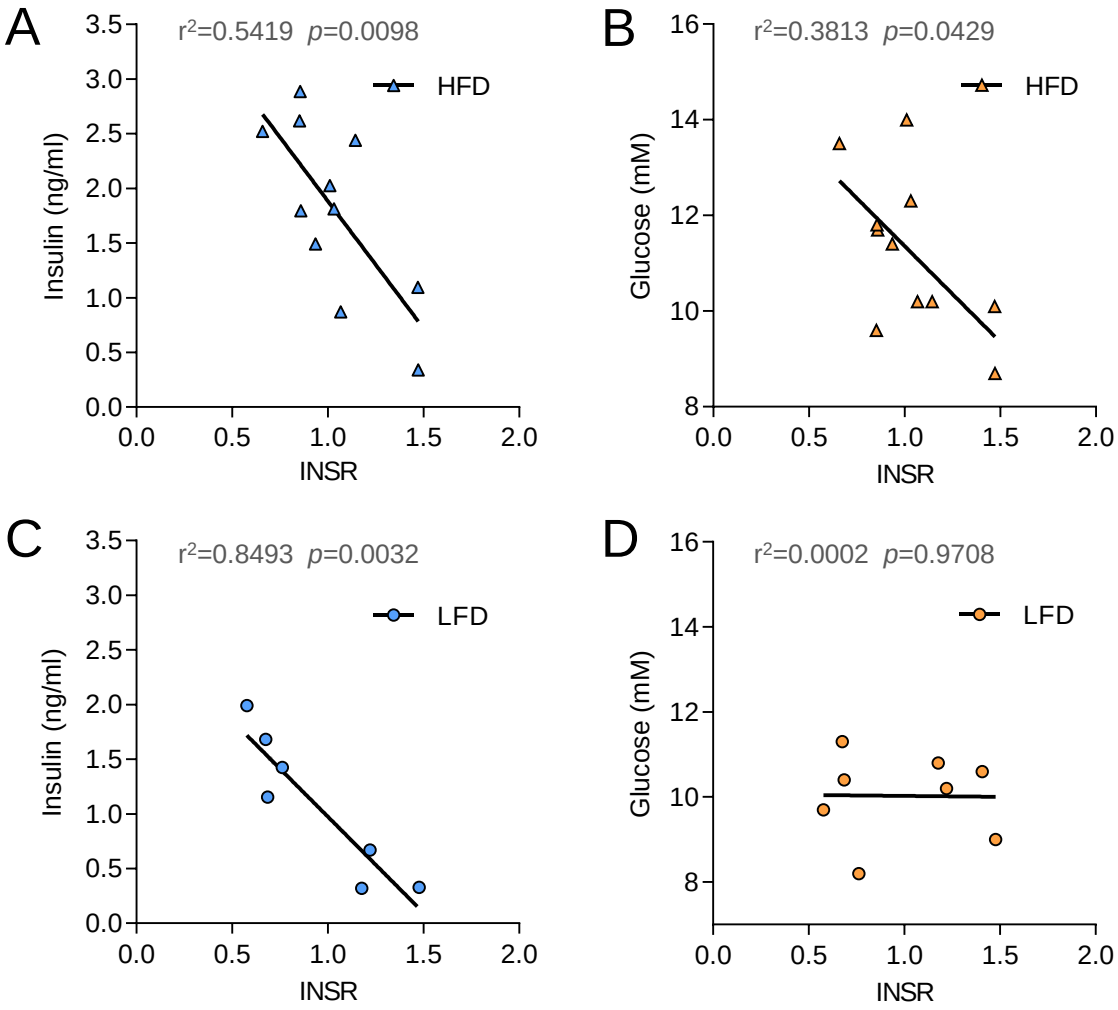

Figure 6. *In vivo* correlation between INSR abundance and fasting insulin or glucose in mouse skeletal muscle.